Physica B 405 (2010) 1022–1032

Contents lists available at ScienceDirect

Physica B

journal homepage: www.elsevier.com/locate/physb

Nearly degenerate electron distributions and superluminal radiation densities

Roman Tomaschitz *

Department of Physics, Hiroshima University, 1-3-1 Kagami-yama, Higashi-Hiroshima 739-8526, Japan

ARTICLE INFO

Article history:
Received 17 June 2009
Accepted 28 October 2009

Keywords:
Fermi power-law ensembles
Nearly degenerate electron plasma
Superluminal radiation
Tachyonic cascade spectra
Spectral curvature
γ-Ray blazars
Negative mass-square
Transversal and longitudinal radiation modes
Polylogarithms

ABSTRACT

Polylogarithmic fugacity expansions of the partition function, the caloric and thermal equations of state, and the specific heat of fermionic power-law distributions are derived in the nearly degenerate low-temperature/high-density quantum regime. The spectral functions of an ultra-relativistic electron plasma are obtained by averaging the tachyonic radiation densities of inertial electrons with Fermi power-laws, whose entropy is shown to be extensive and stable. The averaged radiation densities are put to test by performing tachyonic cascade fits to the γ-ray spectrum of the TeV blazar Markarian 421 in a low and high emission state. Estimates of the thermal electron plasma in this active galactic nucleus are extracted from the spectral fits, such as temperature, number count, and internal energy. The tachyonic cascades reproduce the quiescent as well as a burst spectrum of the blazar obtained with imaging atmospheric Cherenkov detectors. Double-logarithmic plots of the differential tachyon flux exhibit intrinsic spectral curvature, caused by the Boltzmann factor of the electron gas.

1. Introduction

Electronic power-law distributions are commonly used in electromagnetic spectral averages to model the synchrotron emission of astrophysical plasmas, such as the magnetospheric X-ray emission of planets [1]. In this article, we discuss spectral fitting based on fermionic power-law distributions, and develop the thermodynamic formalism of power-law ensembles quantized in Fermi–Dirac statistics. The quasiclassical fugacity expansion pertinent to fermionic power-law distributions in the high-temperature/low-density regime was derived in Ref. [2]. Here, we investigate the opposite asymptotic limit, nearly degenerate ultra-relativistic power-law ensembles in the low-temperature/high-density quantum regime. The efficiency of the spectral averages is demonstrated by applying tachyonic cascade fits to the TeV blazar Mkn 421 in a low emission state and in outburst. The cascade spectra are obtained by averaging the tachyonic radiation densities of individual electrons over ultra-relativistic electron populations in the galactic nucleus. The thermodynamic parameters of the electron plasma are extracted from the spectral fits.

The tachyonic radiation field is a real Proca field with negative mass-square, $(\partial^\nu\partial_\nu + m_t^2)A_\mu = -j_\mu$, subject to the Lorentz condition $A^\mu{}_{,\mu} = 0$, where m_t is the mass of the superluminal Proca field A_μ, and q the tachyonic charge carried by the subluminal electron current $j^\mu = -q\bar{\psi}\gamma^\mu\psi$ [3]. In the Proca equation, the mass term is added with a positive sign, and the sign convention for the d'Alembertian is $\partial^\nu\partial_\nu = \Delta - \partial^2/\partial t^2$, so that $m_t^2 > 0$ is the negative mass-square of the radiation field. The negative mass-square refers to the radiation field rather than the current, in contrast to traditional theories based on superluminal source particles emitting electromagnetic radiation [4–7]. Estimates of the tachyon–electron mass ratio and the tachyonic fine structure constant are $m_t/m \approx 1/238$ and $q^2/(4\pi\hbar c) \approx 1.0 \times 10^{-13}$, obtained from hydrogenic Lamb shifts [8].

Tachyonic radiation implies superluminal signal transfer, the energy quanta propagating faster than light in vacuum, due to their negative mass-square, in contrast to rotating superluminal light sources emitting vacuum Cherenkov radiation [9–14]. This superluminal energy propagation by tachyonic vacuum modes is also to be distinguished from superluminal group velocities arising in photonic crystals, optical fibers, or metamaterials [15–19]. In contrast to tachyonic quanta, the actual signal speed defined by the electromagnetic energy flow in these media is always subluminal and occasionally even opposite to the group velocity [20].

* Tel.: +81 824 247361; fax: +81 824 240717.
E-mail address: tom@geminga.org

0921-4526/$ - see front matter © 2009 Elsevier B.V. All rights reserved.
doi:10.1016/j.physb.2009.10.048

In Section 2, we derive the fugacity expansion of the internal energy and the partition function in the low-temperature/high-density regime. The thermodynamic variables of nearly degenerate power-law distributions are calculated in Section 3, such as the thermal equation of state, entropy, and free energy. We check the positivity of the isochoric heat capacity and the isothermal compressibility for arbitrary power-law index, demonstrating thermodynamic stability in the quantum regime. A generalization of non-relativistic Fermi–Dirac distributions by way of modified dispersion relations has also been suggested in Ref. [21]. Here, we consider ultra-relativistic multi-component plasmas in the collisionless regime [22], in stationary non-equilibrium described by power-law densities [1,23,24].

In Section 4, we study tachyonic radiation densities averaged over electronic power-law distributions, calculate the spectral functions in the nearly degenerate quantum regime, and discuss the range of applicability of the fugacity expansion, including the crossover into the quasiclassical regime. We perform cascade fits to the γ-ray flux of the Markarian galaxy Mkn 421 (at redshift $z\approx 0.031$) in a quiescent state [25] and to a burst spectrum [26], and compare with the tachyonic spectral maps of other BL Lacertae objects. The spectral curvature is reproduced by the tachyonic cascades without resort to intergalactic attenuation mechanisms.

In Section 5, we present our conclusions. In Appendix A, the Sommerfeld asymptotics of incomplete Fermi integrals is derived, which is the basis of the fugacity expansion of the thermodynamic functions in Section 3 and the spectral functions in Section 4. This involves polylogarithms discussed in Appendix B.

2. Ultra-relativistic Fermi power laws

We start with the partition function

$$\log Z=\frac{m^3V}{\pi^2}\int_{\gamma_1}^{\infty}\log\left(1+\gamma^{-\delta}\mathrm{e}^{-\beta\gamma-\alpha}\right)\sqrt{\gamma^2-1}\,\gamma\,\mathrm{d}\gamma, \tag{2.1}$$

of a fermionic power-law density [2]

$$\mathrm{d}\rho_{\mathrm{F}}(\gamma)=\frac{m^3V}{\pi^2}\frac{\sqrt{\gamma^2-1}\,\gamma\,\mathrm{d}\gamma}{1+\gamma^{\delta}\mathrm{e}^{\beta\gamma+\alpha}}, \tag{2.2}$$

where the electronic Lorentz factors range in an interval $\gamma_1\le\gamma<\infty$. γ_1 is the lower edge of Lorentz factors of the electron distribution, the threshold energy being $m\gamma_1$, $\gamma_1\ge 1$. The fugacity exponent α is related to the chemical potential by $\mu=-m\alpha/\beta$. δ is the electronic power-law exponent, and $\beta=m/(kT)$ the cutoff parameter in the Boltzmann factor, so that the Fermi–Dirac equilibrium distribution is recovered with $\delta=0$ and $\gamma_1=1$. Here, we study non-thermal power-law ensembles of arbitrary real power-law index δ. The grand partition function (2.1) is obtained via a standard trace calculation in fermionic occupation number representation. Internal energy and particle number read

$$U=-m\frac{\partial}{\partial\beta}\log Z=\frac{m^4V}{\pi^2}\int_{\gamma_1}^{\infty}\frac{\sqrt{\gamma^2-1}\,\gamma^2\,\mathrm{d}\gamma}{1+\gamma^{\delta}\mathrm{e}^{\beta\gamma+\alpha}}, \tag{2.3}$$

$$N=-\frac{\partial}{\partial\alpha}\log Z=\frac{m^3V}{\pi^2}\int_{\gamma_1}^{\infty}\frac{\sqrt{\gamma^2-1}\,\gamma\,\mathrm{d}\gamma}{1+\gamma^{\delta}\mathrm{e}^{\beta\gamma+\alpha}}. \tag{2.4}$$

Integral representation (2.1) of the partition function $Z(\delta,\beta,\alpha,V)$ is the starting point for the quasiclassical fugacity expansion of the thermodynamic functions, applicable at high temperature and low density [27]. The opposite asymptotic limit, the nearly degenerate quantum regime at low temperature and high density, is based on the representation

$$\log Z=\frac{m^3V}{3\pi^2}\left(\int_{\gamma_1}^{\infty}\frac{(\gamma^2-1)^{3/2}}{1+\gamma^{\delta}\mathrm{e}^{\beta\gamma+\alpha}}\left(\beta+\frac{\delta}{\gamma}\right)\mathrm{d}\gamma-(\gamma_1^2-1)^{3/2}\log\left(1+\gamma_1^{-\delta}\mathrm{e}^{-\beta\gamma_1-\alpha}\right)\right), \tag{2.5}$$

obtained from Eq. (2.1) by partial integration. We replace α by the chemical potential $\mu=-m\alpha/\beta$, and consider U, N, and $\log Z$ as functions of the independent variables μ and β. From now on, we put $\gamma_1=1$. (The case $\gamma_1>1$ will be studied in Section 4.)

The $\mu\to\infty$ asymptotics of the above variables is assembled from the fugacity expansion of the Fermi integrals in Appendix A. The ascending $1/\mu$ series of the particle number reads, cf. Eqs. (A.35) and (A.37),

$$\frac{N}{V}=\frac{\mu^3}{3\pi^2}\left\{1-\frac{3\delta}{\beta}\frac{m}{\mu}\log\frac{\mu}{m}+\frac{3}{\beta^2}\frac{m^2}{\mu^2}\left(\delta^2\log^2\frac{\mu}{m}+\delta^2\log\frac{\mu}{m}+\frac{\pi^2}{3}-\frac{\beta^2}{2}\right)-\frac{3\delta}{\beta^3}\frac{m^3}{\mu^3}\left[\frac{1}{3}\delta^2\log^3\frac{\mu}{m}+\frac{3}{2}\delta^2\log^2\frac{\mu}{m}+\left(\delta^2+\frac{\pi^2}{3}-\frac{\beta^2}{2}\right)\log\frac{\mu}{m}+\frac{\pi^2}{2}\right]+\cdots\right\}. \tag{2.6}$$

The fugacity expansion of the internal energy is obtained from Eqs. (A.36) and (A.37),

$$\frac{U}{V}=\frac{\mu^4}{4\pi^2}\left\{1-\frac{4\delta}{\beta}\frac{m}{\mu}\log\frac{\mu}{m}+\frac{4}{\beta^2}\frac{m^2}{\mu^2}\left(\frac{3}{2}\delta^2\log^2\frac{\mu}{m}+\delta^2\log\frac{\mu}{m}+\frac{\pi^2}{2}-\frac{\beta^2}{4}\right)-\frac{4\delta}{\beta^3}\frac{m^3}{\mu^3}\left[\delta^2\log^3\frac{\mu}{m}+\frac{5}{2}\delta^2\log^2\frac{\mu}{m}+\left(\delta^2+\pi^2-\frac{\beta^2}{2}\right)\log\frac{\mu}{m}+\frac{5}{6}\pi^2\right]+\ldots\right\}, \tag{2.7}$$

and the expansion of the partition function follows from Eq. (A.38):

$$\frac{\log Z}{V}=\frac{\mu^4}{12\pi^2}\frac{\beta}{m}\left\{1-\frac{4\delta}{\beta}\frac{m}{\mu}\left(\log\frac{\mu}{m}-\frac{1}{3}\right)+\frac{4}{\beta^2}\frac{m^2}{\mu^2}\left(\frac{3}{2}\delta^2\log^2\frac{\mu}{m}+\frac{\pi^2}{2}-\frac{3}{4}\beta^2\right)-\frac{4\delta}{\beta^3}\frac{m^3}{\mu^3}\left[\delta^2\log^3\frac{\mu}{m}+\frac{3}{2}\delta^2\log^2\frac{\mu}{m}+\left(\pi^2-\frac{3}{2}\beta^2\right)\log\frac{\mu}{m}+\frac{\pi^2}{2}+\frac{3}{2}\beta^2\right]+\ldots\right\}. \tag{2.8}$$

For these asymptotics to be applicable, conditions $m/\mu\ll 1$ and $m/(\beta\mu)\ll 1$ have to be met. The identities

$$N=\frac{m}{\beta}\frac{\partial}{\partial\mu}\log Z(\mu,\beta),\qquad \frac{U}{m}=\left(\frac{\mu}{\beta}\frac{\partial}{\partial\mu}-\frac{\partial}{\partial\beta}\right)\log Z, \tag{2.9}$$

can be used to check the consistency of series expansions (2.6)–(2.8).

3. Thermodynamic variables of nearly degenerate power-law distributions

The thermodynamic functions are obtained by iteratively solving (2.6) for the chemical potential μ, which is then substituted into the asymptotic series (2.7) and (2.8) of the internal energy and the partition function. Defining the Fermi momentum as $p_{\mathrm{F}}:=(3\pi^2N/V)^{1/3}$, we invert Eq. (2.6) in ascending

powers of $1/p_F$:

$$\mu = p_F\left[1+x\delta\log\frac{p_F}{m}+x^2\left(\frac{\beta^2}{2}-\frac{\pi^2}{3}\right)+x^3\delta\left(\frac{\beta^2}{2}+\frac{\pi^2}{6}\right)+\ldots\right], \tag{3.1}$$

with expansion parameter $x := m/(\beta p_F)$. This is valid for $m/p_F \ll 1$ and $x \ll 1$. The Fermi temperature is defined as the $\beta\to\infty$ limit of $\mu(p_F,\beta)$:

$$kT_F := p_F\left(1+\frac{1}{2}\,\frac{m^2}{p_F^2}+\ldots\right), \qquad \varepsilon_F := \sqrt{p_F^2+m^2} \approx kT_F. \tag{3.2}$$

We substitute $\mu(p_F,\beta)$ into the internal energy (2.7) and partition function (2.8) to find

$$\frac{U}{V} = \frac{p_F^4}{4\pi^2}\left[1+\left(\beta^2+\frac{2}{3}\pi^2\right)x^2-\frac{4}{3}\pi^2\delta x^3+\ldots\right], \tag{3.3}$$

$$\frac{\log Z}{V} = \frac{p_F^4}{12\pi^2}\,\frac{\beta}{m}\left[1+\frac{4}{3}\delta x-\left(\beta^2-\frac{2}{3}\pi^2\right)x^2-4\left(\beta^2+\frac{\pi^2}{3}\right)\delta x^3+\ldots\right]. \tag{3.4}$$

The mean energy per particle in the ultra-relativistic regime is thus $U/N\sim 3p_F/4$. The entropy is calculated via

$$\frac{S}{kN} = \frac{\log Z}{N}+\frac{\beta}{m}\,\frac{U}{N}+\alpha = \frac{3\pi^2}{p_F^3}\left(\frac{\log Z}{V}+\frac{\beta}{m}\frac{U}{V}\right)-\frac{\beta}{m}\mu, \tag{3.5}$$

where we used $N/V = p_F^3/(3\pi^2)$. On substituting series (3.1), (3.3) and (3.4), we obtain

$$\frac{S}{kN} = \left(\frac{1}{3}-\log\frac{p_F}{m}\right)\delta+\pi^2 x-\frac{3}{2}(\beta^2+\pi^2)\delta x^2+\ldots \tag{3.6}$$

The expansion parameter is $x = m/(\beta p_F)$ or

$$x = \frac{1}{3^{1/3}\pi^{2/3}}\,\frac{m}{\beta}\,\frac{V^{1/3}}{N^{1/3}}, \qquad p_F = 3^{1/3}\pi^{2/3}\frac{N^{1/3}}{V^{1/3}}. \tag{3.7}$$

The isochoric heat capacity reads

$$\frac{C_V}{kN} = -\frac{\beta}{kN}\,\frac{\partial S}{\partial\beta} = \pi^2 x(1-3\delta x+\ldots). \tag{3.8}$$

Thermodynamic stability requires $C_V \geq 0$, which is evidently satisfied. The Helmholtz free energy is assembled as

$$F = U-\frac{m}{k\beta}S = V\left(\frac{p_F^3}{3\pi^2}\mu-\frac{m}{\beta}\frac{\log Z}{V}\right), \tag{3.9}$$

where we substitute the fugacity expansions of the chemical potential (3.1) and the partition function (3.4) as well as $V = 3\pi^2 N/p_F^3$ to obtain

$$F(\beta,p_F,N) = \frac{3}{4}Np_F\left[1+\frac{4}{3}\left(\log\frac{p_F}{m}-\frac{1}{3}\right)\delta x+\left(\beta^2-\frac{2}{3}\pi^2\right)x^2+2\left(\beta^2+\frac{\pi^2}{3}\right)\delta x^3+\ldots\right], \tag{3.10}$$

with $x = m/(\beta p_F)$ as in Eq. (3.7). The thermal equation of state

$$P = -\frac{\partial F}{\partial V} = \frac{1}{9\pi^2}\,\frac{p_F^4}{N}\,\frac{\partial}{\partial p_F}F(\beta,p_F,N), \tag{3.11}$$

is thus found as

$$P = \frac{p_F^4}{12\pi^2}\left[1+\frac{4}{3}\delta x-\left(\beta^2-\frac{2}{3}\pi^2\right)x^2-4\left(\beta^2+\frac{\pi^2}{3}\right)\delta x^3+\ldots\right]. \tag{3.12}$$

We solve this equation iteratively for $p_F(\beta,P)$:

$$p_F(\beta,P) = y\left[1-\frac{\delta}{3}\,\frac{m}{\beta y}+\left(\frac{\beta^2}{4}-\frac{\pi^2}{6}+\frac{\delta^2}{6}\right)\frac{m^2}{\beta^2y^2}+\delta\left(\frac{5}{6}\beta^2+\frac{4}{9}\pi^2-\frac{2}{27}\delta^2\right)\frac{m^3}{\beta^3y^3}+\ldots\right], \tag{3.13}$$

where $y := (12\pi^2P)^{1/4}$. The thermal equation (3.12) can thus be written as

$$\frac{N}{V} = \frac{p_F^3(\beta,P)}{3\pi^2} = \frac{y^3}{3\pi^2}\left[1-\delta\frac{m}{\beta y}+\left(\frac{3}{4}\beta^2-\frac{\pi^2}{2}+\frac{5}{6}\delta^2\right)\frac{m^2}{\beta^2y^2}+\delta\left(2\beta^2+\frac{5}{3}\pi^2-\frac{16}{27}\delta^2\right)\frac{m^3}{\beta^3y^3}+\ldots\right]. \tag{3.14}$$

These expansions in ascending powers of $1/y$ are applicable if $m/y \ll 1$ as well as $m/(\beta y)\ll 1$. The isothermal compressibility reads

$$\kappa_T = -\frac{1}{V}\,\frac{\partial V}{\partial P} = 3\frac{\partial}{\partial P}\log p_F(\beta,P), \tag{3.15}$$

where, cf. Eq. (3.13),

$$\log p_F(\beta,P) = \log y-\frac{\delta}{3}\,\frac{m}{\beta y}+\left(\frac{\beta^2}{4}-\frac{\pi^2}{6}+\frac{\delta^2}{9}\right)\frac{m^2}{\beta^2y^2}+\frac{\delta}{6}\left(\frac{11}{2}\beta^2+\frac{7}{3}\pi^2-\frac{5}{27}\delta^2\right)\frac{m^3}{\beta^3y^3}+\ldots, \tag{3.16}$$

so that we arrive at

$$\kappa_T = \frac{3}{4}\,\frac{1}{P}\left[1+\frac{\delta}{3}\,\frac{m}{\beta y}-\left(\frac{\beta^2}{2}-\frac{\pi^2}{3}+\frac{2}{9}\delta^2\right)\frac{m^2}{\beta^2y^2}-\frac{\delta}{2}\left(\frac{11}{2}\beta^2+\frac{7}{3}\pi^2-\frac{5}{27}\delta^2\right)\frac{m^3}{\beta^3y^3}+\ldots\right], \tag{3.17}$$

with $y = (12\pi^2P)^{1/4}$. Thermodynamic stability requires $\kappa_T \geq 0$, which is satisfied.

In the fully degenerate case, at zero temperature, the power-law exponent δ drops out in all thermodynamic variables, and at finite β it does not enter in leading order. The regime below $\beta_F := m/(kT_F)$ is not accessible with the fugacity expansions derived here, which require both $\beta_F \ll 1$ and $\beta_F/\beta \ll 1$. If $\beta \gg 1/\beta_F$, the first-order correction proportional to δ is overpowered by the second order, which is independent of δ in this limit. Therefore, the Chandrasekhar mass limit of white dwarfs is not affected by the power-law exponent, as it assumes total degeneracy [28]. Order-of-magnitude estimates of cooling times derived from homology relations are not affected either, as they are based on the leading-order temperature and density scaling of pressure and specific heat [29].

We have put $\hbar = c = 1$. To restore the dimensions, we rescale $\beta = mc^2/(kT)$ and $p_F = \hbar(3\pi^2N/V)^{1/3}$ so that $kT_F\sim\mu\sim cp_F$, and note $mc^2/k \approx 5.930\times 10^9\,\mathrm{K}$. The expansion parameter $x = mc/(\beta p_F)$ is chosen to be dimensionless, and the dimension of $y = (12\pi^2\hbar^3c^3P)^{1/4}$ to be that of energy. The expansion parameter mc^2/y in Eq. (3.13) is thus dimensionless as well, and $p_F\sim y/c$. Hence

$$\frac{U}{V}\sim 3P\sim\frac{p_F^4c}{4\pi^2\hbar^3}, \qquad \frac{N}{V}\sim\frac{y^3}{3\pi^2\hbar^3c^3}, \tag{3.18}$$

which are the rescaled leading orders of expansions (3.3), (3.12), and (3.14).

4. Tachyonic cascade spectra

The spectral averaging of tachyonic radiation densities with electronic power-law distributions (2.2) has already been explained in Ref. [30], where we mainly focused on the quasiclassical regime, but also derived the general formalism applicable in the nearly degenerate case. In Eqs. (4.1)–(4.5), we summarize the

averaged radiation densities:

$$\langle p^{\mathrm{T,L}}(\omega)\rangle_{\mathrm{F}} = F^{\mathrm{T,L}}(\omega,\gamma_1)\theta(\omega_1-\omega)+F^{\mathrm{T,L}}(\omega,\hat\gamma(\omega))\theta(\omega-\omega_1), \tag{4.1}$$

where the fermionic spectral functions are

$$F^{\mathrm{T,L}}(\omega,\gamma_1)=\frac{\alpha_{\mathrm{q}}m_{\mathrm{t}}^2\omega}{\omega^2+m_{\mathrm{t}}^2}\left[f_3(\gamma_1)-\frac{m_{\mathrm{t}}}{m}\,\frac{\omega}{m_{\mathrm{t}}}f_2(\gamma_1)-\left(\frac14\,\frac{m_{\mathrm{t}}^2}{m^2}+\left(1+\frac{\omega^2}{m_{\mathrm{t}}^2}\right)\Delta^{\mathrm{T,L}}\right)f_1(\gamma_1)\right]. \tag{4.2}$$

The weight factors $f_{k=1,2,3}$ denote the averages

$$f_k(\gamma_1) := \int_{\gamma_1}^{\infty}\frac{\gamma^{k-2}\,\mathrm{d}\rho_{\mathrm{F}}(\gamma)}{\sqrt{\gamma^2-1}} = A_{\mathrm{F}}\int_{\gamma_1}^{\infty}\frac{\gamma^{k-1}\,\mathrm{d}\gamma}{1+\gamma^{\delta}\mathrm{e}^{\beta\gamma+\alpha}}, \tag{4.3}$$

where $A_{\mathrm{F}} := m^3V/\pi^2$ is the normalization factor of the power-law density $\mathrm{d}\rho_{\mathrm{F}}$ in Eq. (2.2). The superscripts T and L in Eq. (4.2) refer to the transversal and longitudinal polarization components defined by $\Delta^{\mathrm{T}}=1-m_{\mathrm{t}}^2/(2m^2)$ and $\Delta^{\mathrm{L}}=0$ [31]. γ is the electronic Lorentz factor, α_{q} the tachyonic fine structure constant, and m_{t} the tachyon mass. The argument $\hat\gamma(\omega)$ in the second spectral function in Eq. (4.1) is the minimal electronic Lorentz factor for radiation at this frequency:

$$\hat\gamma(\omega)=\mu_{\mathrm{t}}\sqrt{1+\frac{\omega^2}{m_{\mathrm{t}}^2}}+\frac12\,\frac{m_{\mathrm{t}}}{m}\,\frac{\omega}{m_{\mathrm{t}}},\qquad \mu_{\mathrm{t}} := \sqrt{1+\frac{m_{\mathrm{t}}^2}{4m^2}}. \tag{4.4}$$

The threshold Lorentz factor γ_1 enters as lower integration boundary in the weights (4.3), and $\gamma_1\geq\mu_{\mathrm{t}}$. In the thermodynamic variables, we can still put $\gamma_1=1$, cf. Eqs. (2.3)–(2.5), but electrons with Lorentz factors below μ_{t} cannot radiate tachyonic quanta [32]. γ_1 determines the break frequency

$$\omega_1 := m_{\mathrm{t}}\left(\mu_{\mathrm{t}}\sqrt{\gamma_1^2-1}-\frac12\,\frac{m_{\mathrm{t}}}{m}\gamma_1\right), \tag{4.5}$$

which enters in the step functions θ in Eq. (4.1), separating the spectrum into a low- and a high-frequency band. In particular, $\hat\gamma(\omega_1)=\gamma_1$, and the smallest possible threshold, $\gamma_1=\mu_{\mathrm{t}}$, corresponds to $\omega_1=0$. The threshold Lorentz factor μ_{t} depends on the tachyon–electron mass ratio, cf. Eq. (4.4), and is not to be confused with the chemical potential μ.

The units $\hbar=c=1$ can easily be restored. We use the Heaviside–Lorentz system, so that $\alpha_{\mathrm{q}}=q^2/(4\pi\hbar c)\approx1.0\times10^{-13}$. The tachyon mass is $m_{\mathrm{t}}\approx2.15\,\mathrm{keV}/c^2$, and the tachyon–electron mass ratio $m_{\mathrm{t}}/m\approx1/238$. These estimates are obtained from hydrogenic Lamb shifts [8]. The particle number reads $N=\int_{\gamma_1}^{\infty}\mathrm{d}\rho_{\mathrm{F}}(\gamma)$, where γ_1 is the lower edge of Lorentz factors in the source population. The exponential cutoff in the spectral weights (4.3) is related to the electron temperature by $\beta=mc^2/(kT)$ and the chemical potential by $\mu=-m\alpha/\beta$. The normalization factor A_{F} is dimensionless via $m\to mc/\hbar$; the volume factor in the thermodynamic functions in Section 3 is thus found as $V=\pi^2\lambda\!\!\!^{-3}_{\mathrm{e}}A_{\mathrm{F}}$, where $\lambda\!\!\!^{-}_{\mathrm{e}}\approx386\,\mathrm{fm}$ is the reduced electronic Compton wavelength.

The weight factors (4.3) are related to the Fermi integral $F(a,b)$ in Eq. (A.1) (with $a=k-1$ and b=0) and the Sommerfeld decomposition (A.3) by

$$f_k(\gamma_1)=A_{\mathrm{F}}F(k-1,0)=A_{\mathrm{F}}\gamma^k(F_0+F_1+F_2), \tag{4.6}$$

with normalization A_{F} as in Eq. (4.3). We substitute $F_0(k-1,0)=(z^k-1)/k$, cf. Eq. (A.33), and assemble the temperature dependent contribution F_1+F_2 in Eq. (4.6) by making use of Eqs. (A.19)–(A.22) (with $a=k-1$ and b=0),

$$\begin{aligned}F_1+F_2=&-z^k\left\{\frac{\delta\log z}{z\beta\gamma_1}-\frac{1}{(z\beta\gamma_1)^2}\left[(k-1)\left(\frac{\delta^2}{2}\log^2z+\frac{\pi^2}{6}\right)+\delta^2\log z\right]\right.\\&+\frac{\delta}{(z\beta\gamma_1)^3}\left[(k-1)(k-2)\left(\frac{\delta^2}{6}\log^3z+\frac{\pi^2}{6}\log z\right)\right.\\&\left.\left.+(2k-3)\left(\frac{\delta^2}{2}\log^2z+\frac{\pi^2}{6}\right)+\delta^2\log z\right]+\ldots\right\}.\end{aligned} \tag{4.7}$$

The expansion parameter z is defined in Eq. (A.20):

$$z=-\frac{\alpha+\delta\log\gamma_1}{\beta\gamma_1}=\frac{\mu}{m\gamma_1}-\frac{\delta\log\gamma_1}{\beta\gamma_1}, \tag{4.8}$$

where μ is the chemical potential, cf. after Eq. (4.5). For the asymptotic series (4.7) to be applicable, conditions $\beta\gamma_1z\gg1$ as well as $z>1$ have to be satisfied. [Since b=0, we do not need to require $\gamma_1z\gg1$, even though series (4.7) is a systematic ascending $1/z$ expansion, cf. Eq. (A.23) and after Eq. (A.34). In fact, F_0 is a polynomial in z, and the factor $\rho(\gamma_1z)$ in Eq. (A.21) drops out in F_1+F_2 at b=0, cf. Eqs. (A.13) and (A.15), so that an additional temperature independent expansion in inverse powers of γ_1z is not needed if b=0 in the Fermi integral (A.1).]

The amplitude A_{F} and the fugacity $\mathrm{e}^{-\alpha}$ are two independent fitting parameters in the source density $\mathrm{d}\rho_{\mathrm{F}}(\gamma)$, cf. Eqs. (2.2) and (4.3). This is in contrast to the classical limit, $\mathrm{d}\rho_{\mathrm{F}}\sim A_{\mathrm{F}}\mathrm{e}^{-\alpha}\gamma^{1-\delta}\mathrm{e}^{-\beta\gamma}\sqrt{\gamma^2-1}\,\mathrm{d}\gamma$, where the factors of the amplitude $A_{\mathrm{F}}\mathrm{e}^{-\alpha}$ cannot independently be determined from the spectral fit. This amplitude differs from a classical Boltzmann power-law distribution due to the fermionic multiplicity factor, the Boltzmann normalization being $A_{\mathrm{F}}\mathrm{e}^{-\alpha}/2$, cf. Eq. (3.7) in Ref. [24]. In the ultra-relativistic limit, $\gamma\gg1$, the factor $\gamma^{-\delta}$ can formally be generated by analytic continuation in the momentum space dimension, since $p\sim m\gamma$ [33]. In the case of a genuine fermionic power-law distribution in the nearly degenerate quantum regime, one can determine the volume as well as the particle number from the spectral fit, cf. after Eq. (4.5).

We parametrize the spectral weights $f_k(\gamma_1)$ with the chemical potential via $z(\mu)$ in Eq. (4.8). The independent fitting parameters in $f_k(\gamma_1)$ are thus temperature β, threshold Lorentz factor γ_1, chemical potential μ, and the volume factor A_{F} of the Fermi distribution in Eq. (4.3). We may fix γ_1 at the lowest possible threshold, $\gamma_1=\mu_{\mathrm{t}}$, cf. Eq. (4.4) (and put $\gamma_1=1$ in the thermodynamic functions (2.3)–(2.5)), so that the averaged spectral densities (4.1) simplify to

$$\langle p^{\mathrm{T,L}}(\omega)\rangle_{\mathrm{F}}=F^{\mathrm{T,L}}(\omega;\hat\gamma(\omega)). \tag{4.9}$$

The expansion parameter $z(\mu)$ in Eq. (4.8) becomes frequency dependent via the substitution $\gamma_1=\hat\gamma(\omega)$, required in densities (4.9). The condition $z>1$ for the fugacity expansion (4.7) to apply is violated at sufficiently large ω, cf. Eq. (4.4). In this case, or if condition $\beta\gamma_1z\gg1$ is not met, the asymptotic series of F_1+F_2 in Eq. (4.7) breaks down, so that we have to switch to the exact integral representation (4.3) of the weight factors $f_k(\gamma_1)$, and numerically integrate the crossover into the quasiclassical regime. The quasiclassical fugacity expansion [2] can be used if

$$\hat\gamma^{-\delta}(\omega)\mathrm{e}^{-\beta\hat\gamma(\omega)-\alpha}=\mathrm{e}^{-(1-z)\beta\hat\gamma(\omega)}\ll1, \tag{4.10}$$

which allows to expand the denominator in Eq. (2.2) to arrive in leading order at the classical power-law density, cf. after Eq. (4.8),

$$\mathrm{d}\rho_{\hat\alpha,\beta}(\gamma)=A_{\hat\alpha,\beta}\gamma^{-\hat\alpha-1}\mathrm{e}^{-\beta\gamma}\sqrt{\gamma^2-1}\,\mathrm{d}\gamma. \tag{4.11}$$

Here, we use the customary definition of the electronic power-law index, $\hat\alpha=\delta-2$. (The electron index $\hat\alpha$ is denoted by a hat, to avoid confusion with the parameter α in Eq. (4.10) defining the fugacity $\mathrm{e}^{-\alpha}$ and the chemical potential.) The normalization factor $A_{\hat\alpha,\beta}$ is related to the particle number via $N=\int_{\gamma_1}^{\infty}\mathrm{d}\rho_{\hat\alpha,\beta}(\gamma)$ to be identified with the renormalized electron count n^{e} obtained from the spectral fit, cf. after Eq. (4.15). The cascades $\rho_{i=1,2}$ depicted in Figs. 1 and 2 are generated with $\hat\alpha=-2$ and $\gamma_1=1$, that is, with Maxwell–Boltzmann distributions as specified in Table 1. Condition (4.10) can even be met at high temperature, at sufficiently high frequency, cf. Eq. (4.4), implying exponential decay of the spectral functions $f_k(\hat\gamma(\omega))$.

The classical limit of the fermionic spectral functions $F^{\mathrm{T,L}}(\omega,\gamma_1)$ is the Boltzmann average $B^{\mathrm{T,L}}(\omega,\gamma_1)$, obtained by dropping all terms containing m_{t}/m factors in Eq. (4.2), and replacing $\mathrm{d}\rho_{\mathrm{F}}$ in the spectral weights (4.3) by the classical density $\mathrm{d}\rho_{\hat{\alpha},\beta}$ in Eq. (4.11). The classical spectral weights reduce to incomplete gamma functions. Terms containing m_{t}/m factors in Eqs. (4.4) and (4.5) are dropped as well, and the polarization coefficients reduce to $\Delta_{\mathrm{cl}}^{\mathrm{T}}=1$ and $\Delta_{\mathrm{cl}}^{\mathrm{L}}=0$, cf. after Eq. (4.3). The classical limit of the averaged spectral densities $\langle p^{\mathrm{T,L}}(\omega)\rangle_{\mathrm{F}}$ in Eq. (4.1) thus reads

$$\langle p^{\mathrm{T,L}}(\omega)\rangle_{\hat{\alpha},\beta}=B^{\mathrm{T,L}}(\omega,\gamma_1)\theta(\omega_{1,\mathrm{cl}}-\omega)+B^{\mathrm{T,L}}(\omega,\sqrt{1+\omega^2/m_{\mathrm{t}}^2})\theta(\omega-\omega_{1,\mathrm{cl}}),$$

$$B^{\mathrm{T,L}}(\omega,\gamma_1):=A_{\hat{\alpha},\beta}\frac{\alpha_{\mathrm{q}}m_{\mathrm{t}}^2\omega}{\omega^2+m_{\mathrm{t}}^2}\beta^{\hat{\alpha}-1}\left[\Gamma(1-\hat{\alpha},\beta\gamma_1)-\left(1+\frac{\omega^2}{m_{\mathrm{t}}^2}\right)\Delta_{\mathrm{cl}}^{\mathrm{T,L}}\beta^2\Gamma(-1-\hat{\alpha},\beta\gamma_1)\right], \tag{4.12}$$

where the argument $\omega_{1,\mathrm{cl}}:=m_{\mathrm{t}}\sqrt{\gamma_1^2-1}$ in the step functions is the classical limit of the break frequency (4.5).

The spectral fits of the BL Lacertae object (BL Lac) Markarian 421 in Figs. 1 and 2 are based on the E^2-rescaled flux densities [34]

$$E^2\frac{\mathrm{d}N^{\mathrm{T,L}}}{\mathrm{d}E}=\frac{\omega}{4\pi d^2}\langle p^{\mathrm{T,L}}(\omega)\rangle_{\hat{\alpha},\beta}, \tag{4.13}$$

where d is the distance to the galaxy and $\langle p^{\mathrm{T,L}}(\omega)\rangle_{\hat{\alpha},\beta}$ the spectral average (4.12). The cascade fits are performed with the unpolarized flux density $\mathrm{d}N^{\mathrm{T+L}}=\mathrm{d}N^{\mathrm{T}}+\mathrm{d}N^{\mathrm{L}}$ of thermal electron populations (4.11) ($\hat{\alpha}=-2$, $\gamma_1=1$). Each electron density generates a cascade ρ_i, and the spectral map is obtained by adding two cascade spectra labeled $\rho_{1,2}$ in the figures. As for the electron count

$$n_1:=\int_1^\infty \mathrm{d}\rho_{\hat{\alpha},\beta}(\gamma), \tag{4.14}$$

we use a rescaled parameter $\hat{n}$ for the fit,

$$\hat{n}:=\frac{\alpha_{\mathrm{q}}n_1}{\hbar\,[\mathrm{keV\,s}]4\pi d^2\,[\mathrm{cm}]}\approx 1.27\times 10^{-45}\frac{n_1}{d^2\,[\mathrm{Mpc}]}, \tag{4.15}$$

which is independent of the distance estimate in Eq. (4.13). Here, $\hbar\,[\mathrm{keV\,s}]$ implies the tachyon mass in keV units in the spectral functions (4.12). At γ-ray energies, only a tiny $\alpha_{\mathrm{q}}/\alpha_{\mathrm{e}}$ fraction (the ratio of tachyonic and electric fine structure constants) of the tachyon flux is absorbed by the detector, which requires a rescaling of the electron count n_1, so that the actual number of radiating electrons is $n^{\mathrm{e}}:=n_1\alpha_{\mathrm{e}}/\alpha_{\mathrm{q}}\approx 7.3\times 10^{10}n_1$. We thus find the electron count as $n^{\mathrm{e}}\approx 5.75\times 10^{55}\hat{n}d^2\,[\mathrm{Mpc}]$, where $\hat{n}$ defines the tachyonic flux amplitude extracted from the spectral fit [3]. This renormalized count n^{e} is to be identified with the particle number N in the thermodynamic variables. The electron temperature and cutoff parameter in the Boltzmann factor are related by $kT\,[\mathrm{TeV}]\approx 5.11\times 10^{-7}/\beta$, and the energy estimates in Table 1

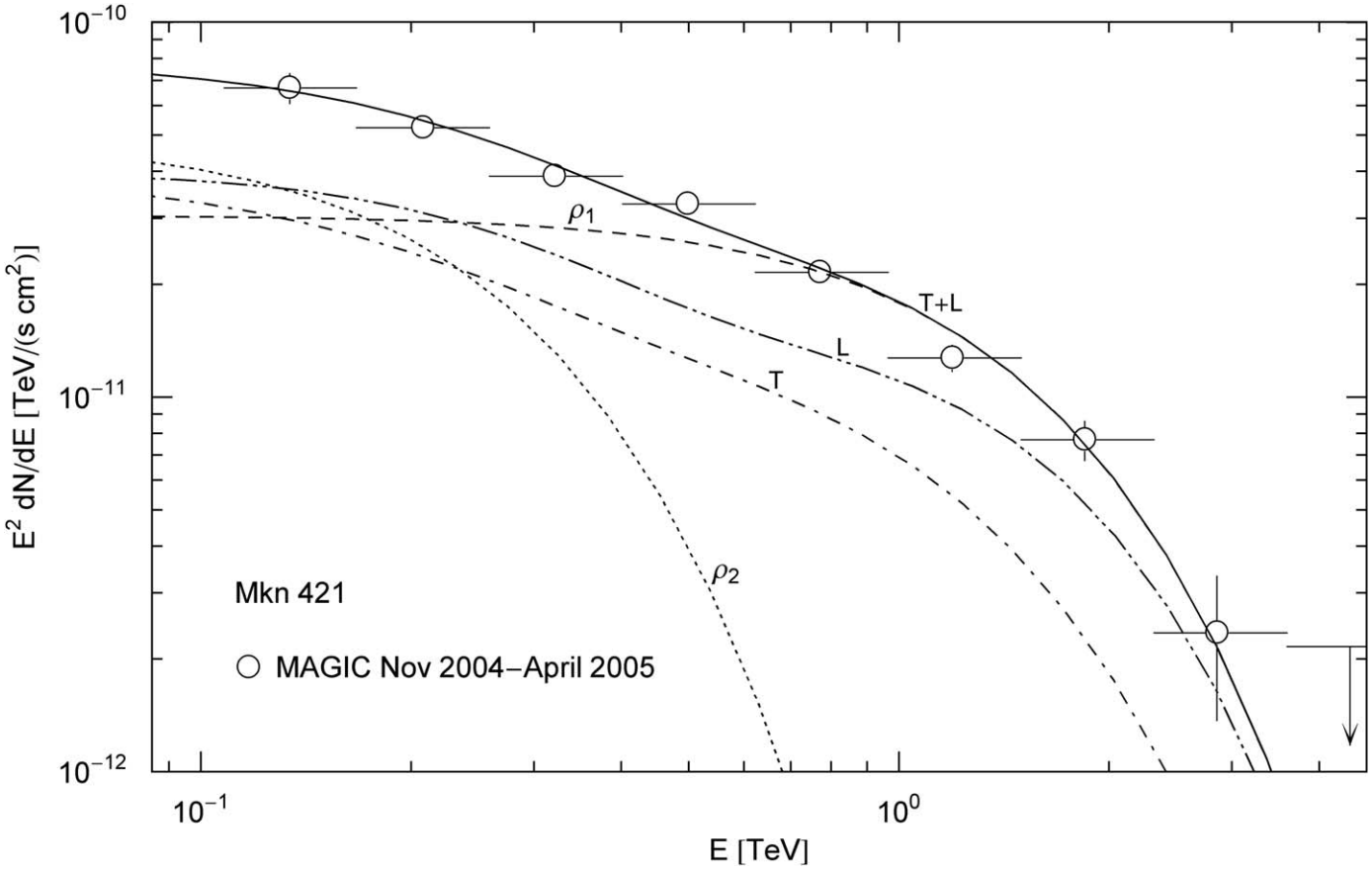

Fig. 1. Spectral map of the Markarian blazar Mkn 421 in a low emission state. MAGIC flux points from Ref. [25]. The solid line T+L depicts the unpolarized differential tachyon flux $\mathrm{d}N^{\mathrm{T+L}}/\mathrm{d}E$, obtained by adding the flux densities $\rho_{1,2}$ of two ultra-relativistic electron populations, cf. Table 1, and rescaled with E^2 for better visibility of the spectral curvature, cf. Eq. (4.13). The transversal and longitudinal flux densities $\mathrm{d}N^{\mathrm{T,L}}/\mathrm{d}E$ add up to the total flux $\mathrm{T+L}=\rho_1+\rho_2$. The exponential decay of the cascades $\rho_{1,2}$ sets in at about $E_{\mathrm{cut}}\approx(m_{\mathrm{t}}/m)kT$, where $m_{\mathrm{t}}/m\approx 1/238$ is the tachyon–electron mass ratio [8], implying cutoff energies of 550 GeV for the ρ_1 cascade and 100 GeV for ρ_2. The spectral curvature resembles that of the TeV blazar W Comae in Fig. 2 of Ref. [27] at 450 Mpc, which suggests the curvature to be intrinsic rather than due to intergalactic absorption. One may also compare this cascade spectrum to the spectral maps of the BL Lacs 1ES 0347–212 at 830 Mpc, cf. Fig. 2 of Ref. [30], and 1ES 1218+304 at 800 Mpc, cf. Fig. 2 of Ref. [3]. There is no correlation of redshift and spectral curvature visible.

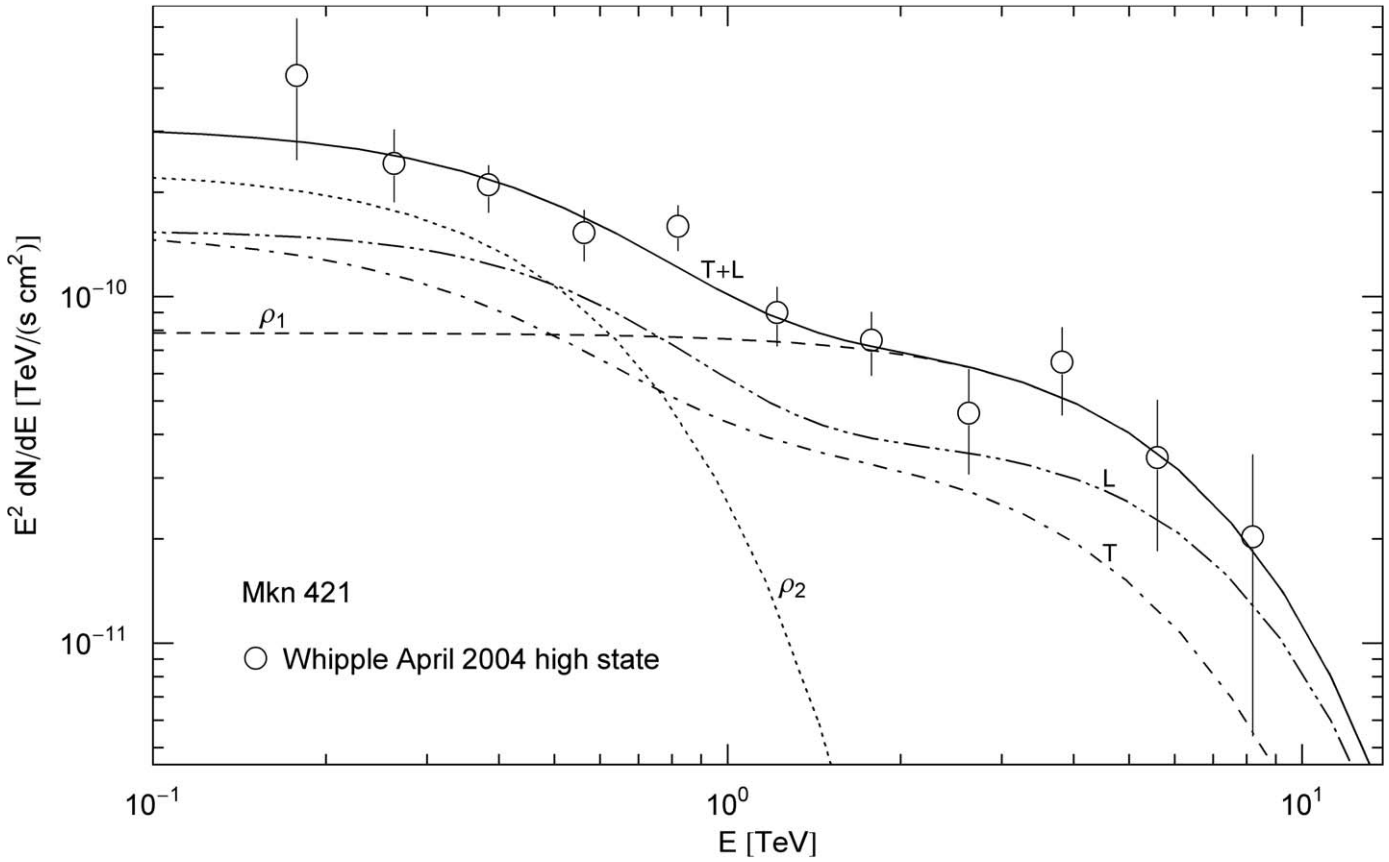

Fig. 2. Spectral map of Mkn 421 in a high state. Whipple data points from Ref. [26], notation as in Fig. 1. T and L stand for the transversal and longitudinal flux components, and T+L is the unpolarized cascade fit. Temperature and number count of the ultra-relativistic electron populations generating the cascades $\rho_{1,2}$ are recorded in Table 1. The cutoff energy is 2.4 TeV for the ρ_1 cascade and 220 GeV for ρ_2. The spectral curvature of the rescaled flux density $E^2\,\mathrm{d}N^{\mathrm{T+L}}/\mathrm{d}E$ is generated by the Boltzmann factor of the thermal electron populations, cf. Table 1, and the spectral map differs from the quiescent state in Fig. 1 beyond a simple rescaling. This suggests that the curvature of the plotted flux density is intrinsic rather than depending on distance. The high-energy cascade is comparable to the HESS spectrum of the same outburst in April 2004, cf. Fig. 6 in Ref. [31]. One may also compare Figs. 1 and 2 to the spectral slope of BL Lac 1ES 2344+514 in Fig. 3 of Ref. [27], which has a similar redshift but a more pronounced spectral curvature. Conversely, the redshift of BL Lac PG 1553+113 in Fig. 4 of Ref. [27] is higher by almost a factor of 10, although this blazar has a spectral slope similar to that of the depicted high state. Even the cascade fit of the Galactic γ-ray binary LS 5039 in Fig. 3 of Ref. [30] is more strongly curved than of Mkn 421 in this figure. The spectral curvature is thus uncorrelated with distance. The tachyonic γ-ray cascades of Mkn 421 as well as of the BL Lacs mentioned in the captions are generated by thermal electron distributions, and the spectral fits extend into the lower GeV region as spectral plateaus. By contrast, non-thermal cascades generated by the shock-heated electron plasmas of supernova remnants [38] exhibit a slightly curved or straight power-law crossover ($E^2\,\mathrm{d}N/\mathrm{d}E \propto E^{1-\hat{\alpha}}$ for electron indices $\hat{\alpha} > 1$, cf. Eqs. (4.11) and (4.13)) between the spectral plateau and the exponentially decaying slope, absent in the thermal spectra of active galactic nuclei.

Table 1
Thermal electronic source distributions ρ_i generating the tachyonic γ-ray cascades of the Markarian galaxy Mkn 421.

Markarian 421 $z \approx 0.031$, 140 Mpc	β	$\hat{n}$	n^{e}	kT (TeV)	U (10^{60} erg)
MAGIC, November 2004–April 2005					
ρ_1	3.91×10^{-9}	3.3×10^{-3}	3.5×10^{57}	131	2.2
ρ_2	2.15×10^{-8}	5.3×10^{-3}	5.6×10^{57}	23.8	0.64
Whipple, April 2004					
ρ_1	8.96×10^{-10}	8.5×10^{-3}	9.0×10^{57}	570	25
ρ_2	9.77×10^{-9}	2.5×10^{-2}	2.7×10^{58}	52.3	6.7

Each ρ_i stands for a Maxwell–Boltzmann density $\mathrm{d}\rho_{\hat{\alpha}=-2,\beta}(\gamma)$ as defined in Eq. (4.11) (with $\delta = 0$ and $\gamma_1 = 1$). β is the cutoff parameter in the Boltzmann factor, and $\hat{n}$ determines the amplitude of the tachyon flux generated by density ρ_i, from which the electron count $n^{\mathrm{e}} \propto d^2$ is inferred at the indicated distance. kT is the temperature and U the internal energy of the electron populations, cf. after Eq. (4.15). Each cascade depends on two fitting parameters β and $\hat{n}$ extracted from the χ^2 fit $\mathrm{T+L} = \rho_1 + \rho_2$ in Figs. 1 and 2. The tachyonic cascades labeled $\rho_{1,2}$ in the figures are produced by the corresponding electron densities listed in this table.

are based on $U[\mathrm{erg}] \sim 2.46 \times 10^{-6} n^{\mathrm{e}}/\beta$ [35]. The distance in Eq. (4.13) is inferred from the redshift via $d \sim cz/H_0$, with $c/H_0 \approx 4.4 \times 10^3$ Mpc, that is, $h_0 \approx 0.68$. Hence, $d[\mathrm{Mpc}] \approx 4.4 \times 10^3 z$, and $n^{\mathrm{e}} \approx 1.1 \times 10^{63} \hat{n} z^2$. The distance estimate does not affect the spectral maps, but the electron number n^{e}.

Fig. 1 shows the cascade fit of the Markarian galaxy Mkn 421 in a quiescent state [25], and Fig. 2 in a high emission state [26]. The redshift of Mkn 421 is $z \approx 0.031$, implying a distance of 140 Mpc. TeV γ-ray spectra of active galactic nuclei are usually assumed to be generated by inverse Compton scattering or *pp* scattering followed by pion decay. Both mechanisms result in a flux of TeV photons, assumed to be partially absorbed by interaction with background photons due to pair creation, so that the intrinsic spectrum has to be reconstructed on the basis of intergalactic

absorption models depending on vaguely known cosmological input parameters. In contrast, the extragalactic tachyon flux is not attenuated by interaction with the background light, there is no absorption of tachyonic γ-rays. The curvature of the γ-ray spectra in double-logarithmic plots is caused by the Boltzmann factor of the electron densities generating the tachyon flux, so that the observed spectrum is already the intrinsic one, and no reconstruction is needed. The curvature present in the γ-ray spectra of BL Lacs is not correlated with distance; the spectral curvature does not increase with redshift if we compare the spectral fits in Figs. 1 and 2 to the spectral maps of other active galactic nuclei, cf. the figure captions.

5. Conclusion

Tachyonic γ-ray spectra of active galactic nuclei are generated by ultra-relativistic electron populations. Tachyons are radiation modes, unrelated to electromagnetic radiation. Electrons radiate tachyons, and these tachyonic quanta produce the observed γ-ray cascades. The tachyonic radiation modes are coupled by minimal substitution to the electron current. This field theory, a real Proca field with negative mass-square, admits a static potential analogous to the Coulomb potential, but oscillating because of the negative mass-square, and much weaker due to the small tachyonic fine structure constant. In the spectral maps, the tachyon–electron mass ratio shows in the cutoff energy of the cascades. The negative mass-square of tachyons implies superluminal velocity and allows longitudinal polarization. The tachyonic radiation field does not couple to electromagnetic fields, nor is it affected by electric charge. Thus, interaction of tachyons with photons can only happen indirectly via matter fields. In contrast to electromagnetic γ-rays, there is no extinction of the extragalactic tachyon flux by the cosmic background light, as tachyons do not interact with infrared photons. The ultra-relativistic electron plasma in the active galactic nucleus produces tachyonic γ-rays propagating unattenuated over intergalactic distances.

The tachyonic radiation density averaged over the electron populations in the galactic nucleus is generated by electrons in uniform motion. In particular, there is no electromagnetic radiation damping, as photons can only be radiated by accelerated charges, in contrast to tachyonic quanta, where the emission rate primarily depends on the electronic Lorentz factor rather than on acceleration [3]. The high plasma temperature inferred from the spectral fits implies ultra-high energy electrons. Such high electron temperatures are also found in Galactic pulsar wind nebulae, production sites of ultra-high energy cosmic rays [36].

Specifically, we fitted a quiescent as well as a flare spectrum of the γ-ray blazar Mkn 421 with tachyonic cascades, and found that the spectral curvature is intrinsic and reproduced by the superluminal spectral densities (4.1) averaged with ultra-relativistic electron distributions. The curvature present in the γ-ray spectra of active galactic nuclei is not correlated with distance, so that absorption of electromagnetic radiation due to interaction with background photons is not a viable explanation for the spectral curvature. By contrast, there is no intergalactic attenuation of the tachyon flux, as tachyons cannot interact with photons. In Table 1, we have given estimates of the temperature, the source count, and the internal energy of the electron populations in the galactic nucleus generating the superluminal γ-ray cascades.

The fugacity expansion of the thermodynamic variables of a nearly degenerate electron plasma was derived in Sections 2 and 3, and fermionic power-law densities were shown to admit a stable and extensive entropy function in the quantum regime, cf. Eqs. (3.5) and (3.6). In Section 4, we averaged tachyonic spectral densities with electronic power-law distributions, and obtained the fugacity expansion of the quantized spectral functions in the nearly degenerate low-temperature/low-frequency/high-density regime. The integral representation (4.3) of the spectral weights covers the crossover into the quasiclassical high-temperature/high-frequency/low-density regime studied in Ref. [2].

Superluminal radiation from ultra-relativistic electrons orbiting in magnetic fields was investigated in Ref. [37]. In the zero-magnetic-field limit, the averaged tachyonic synchrotron densities converge to the spectral densities (4.12). Orbital curvature induces modulations in the spectral slopes, but these ripples are attenuated when performing a pitch-angle average, cf. Figs. 1–3 of Ref. [37]. Thus we can use uniform radiation densities even in the presence of magnetic fields in the galactic nuclei.

Acknowledgments

The author acknowledges the support of the Japan Society for the Promotion of Science. The hospitality and stimulating atmosphere of the Centre for Nonlinear Dynamics, Bharathidasan University, Trichy, and the Institute of Mathematical Sciences, Chennai, are likewise gratefully acknowledged.

Appendix A. Incomplete integrals of fermionic power-law densities

The thermodynamic variables in Eqs. (2.3)–(2.5) are composed of integrals of type

$$F(a,b) := \int_{\gamma_1}^{\infty} \frac{\gamma^a(\gamma^2-1)^{b/2}}{\Lambda_0^{-1}\gamma^\delta \mathrm{e}^{\beta\gamma}+1}\,\mathrm{d}\gamma, \tag{A.1}$$

where $\Lambda_0 := \mathrm{e}^{-\alpha}$ denotes the fugacity. We derive the $\Lambda_0\to\infty$ asymptotics of this integral, with lower integration boundary $\gamma_1\geq 1$ and real parameters $\Lambda_0>0$, $\beta>0$. The exponents a and b are moderate real numbers, and so is the power-law exponent δ. If the integral is complete, $\gamma_1=1$, we have to require $b>-2$ for convergence.

We perform the substitution $\gamma=\gamma_1(1+y)$ in Eq. (A.1),

$$F=\gamma_1^{a+1}\int_0^\infty \frac{f(y)\,\mathrm{d}y}{\Lambda^{-1}(1+y)^\delta \mathrm{e}^{\beta\gamma_1 y}+1}, \qquad \Lambda := \gamma_1^{-\delta}\mathrm{e}^{-\beta\gamma_1}\Lambda_0,$$

$$f(y) := (1+y)^a[\gamma_1^2(1+y)^2-1]^{b/2}, \tag{A.2}$$

and use the Sommerfeld decomposition [39]:

$$F=\gamma_1^{a+1}(F_0+F_1+F_2),$$

$$F_0 := \int_0^\lambda f(y)\,\mathrm{d}y, \qquad F_1 := -\int_0^\lambda \frac{f(y)\,\mathrm{d}y}{1+\Lambda(1+y)^{-\delta}\mathrm{e}^{-\beta\gamma_1 y}},$$

$$F_2 := \int_\lambda^\infty \frac{f(y)\,\mathrm{d}y}{\Lambda^{-1}(1+y)^\delta \mathrm{e}^{\beta\gamma_1 y}+1}, \qquad \lambda := \frac{\log\Lambda}{\beta\gamma_1}. \tag{A.3}$$

The asymptotics of the temperature-dependent contribution F_1+F_2 is discussed below, and the zero-temperature degeneracy F_0 in Section A.2.

A.1. Fugacity expansion at low temperature and high density

The ascending $1/\log\Lambda$ expansion of F_1+F_2 in Eq. (A.3) is found by means of the substitutions $y=\lambda(1-t)$ in F_1 and $y=\lambda(1+t)$ in F_2. Expanding the denominator in powers of $\mathrm{e}^{-t\log\Lambda}$, we obtain

$$F_1=\lambda\sum_{k=1}^\infty(-1)^k\int_0^1 \mathrm{e}^{-tk\log\Lambda}g_k(t,\delta,\lambda)\,\mathrm{d}t, \tag{A.4}$$

$$F_2=\lambda\sum_{k=1}^{\infty}(-1)^{k+1}\int_0^{\infty}\mathrm{e}^{-tk\log\Lambda}g_k(-t,-\delta,\lambda)\,\mathrm{d}t, \tag{A.5}$$

$$g_k(t,\delta,\lambda):=f(\lambda(1-t))(1+\lambda(1-t))^{k\delta}, \tag{A.6}$$

where $f(y)$ is defined in Eq. (A.2). In F_1, we extend the upper integration boundary to infinity, which is justified by Watson's lemma, as the error is of order $\mathrm{O}(1/\Lambda)$, as compared to the expansion in powers of $1/\log\Lambda$. We can replace the upper integration boundaries in Eqs. (A.4) and (A.5) by an arbitrary ε, since the asymptotic series is determined by the Taylor coefficients of $g_k(t,\delta,\lambda)$ at $t=0$:

$$g_k(t,\delta,\lambda)=\sum_{n=0}^{\infty}a_{k,n}(\delta,\lambda)t^n, \tag{A.7}$$

and does not depend on the upper integration boundary if terms of $\mathrm{O}(1/\Lambda)$ are neglected [40]. For technical convenience, we extend the integration boundaries to infinity, even though series (A.7) may only have a small radius of convergence, cf. Eq. (B.17). (In this way, we avoid incomplete gamma functions in the term-by-term integrations in Eqs. (A.4) and (A.5), which would have to be expanded to arrive at series (A.8) and (A.9) below.) On substituting series (A.7) into Eqs. (A.4) and (A.5), and interchanging integration and summations, we find

$$F_1\sim\lambda\sum_{n=0}^{\infty}\frac{\Gamma(n+1)}{\log^{n+1}\Lambda}\sum_{k=1}^{\infty}(-1)^k\frac{a_{k,n}(\delta,\lambda)}{k^{n+1}}, \tag{A.8}$$

$$F_2\sim\lambda\sum_{n=0}^{\infty}(-1)^{n+1}\frac{\Gamma(n+1)}{\log^{n+1}\Lambda}\sum_{k=1}^{\infty}(-1)^k\frac{a_{k,n}(-\delta,\lambda)}{k^{n+1}}. \tag{A.9}$$

To obtain the Taylor coefficients $a_{k,n}(\delta,\lambda)$ in Eq. (A.7), we factorize $g_k(t,\delta,\lambda)=h_1h_2$, cf. Eqs. (A.2) and (A.6),

$$h_1:=(1+\lambda-\lambda t)^{k\delta+a},\qquad h_2:=(\gamma_1^2(1+\lambda-\lambda t)^2-1)^{b/2}, \tag{A.10}$$

and expand both factors. The Taylor series of h_1 reads

$$h_1=(1+\lambda)^{k\delta+a}\sum_{m=0}^{\infty}(-1)^m\frac{(k\delta+a)_m}{m!}\frac{\lambda^m t^m}{(1+\lambda)^m}. \tag{A.11}$$

As for h_2, we introduce the shortcuts

$$\rho:=\frac{\gamma_1(1+\lambda)}{\sqrt{\gamma_1^2(1+\lambda)^2-1}},\qquad \tilde{t}:=\frac{\lambda\rho t}{\lambda+1}, \tag{A.12}$$

and find, by means of the Gegenbauer expansion (B.17):

$$\begin{aligned}h_2&=\gamma_1^b\rho^{-b}(1+\lambda)^b(1-2\rho\tilde{t}+\tilde{t}^2)^{b/2}\\&=\gamma_1^b\rho^{-b}(1+\lambda)^b\sum_{l=0}^{\infty}\rho^l C_l^{(-b/2)}(\rho)\frac{\lambda^l t^l}{(1+\lambda)^l}.\end{aligned} \tag{A.13}$$

We replace the binomial coefficient $(k\delta+a)_m/m!$ in Eq. (A.11) by the Stirling expansion (B.14), and use the product of series (A.11) and (A.13) to find the Taylor coefficients of $g_k(t,\delta,\lambda)$ in Eq. (A.7) as

$$a_{k,n}(\delta,\lambda)=(1+\lambda)^{k\delta}\sum_{m=0}^{n}\alpha_{n,m}(\lambda)\delta^m k^m, \tag{A.14}$$

$$\alpha_{n,m}(\lambda):=(-\lambda)^n(1+\lambda)^{a+b-n}\gamma_1^b\rho^{-b}\sum_{l=0}^{n-m}(-\rho)^l C_l^{(-b/2)}(\rho)S(n-l,m;a). \tag{A.15}$$

The coefficients $S(n,m;a)$ are calculated in Eqs. (B.15) and (B.16), and we put $\alpha_{n,m}(\lambda)=0$ for $m>n$. The Gegenbauer polynomials $C_l^{(-b/2)}(\rho)$ are listed in Eqs. (B.18)–(B.20). We substitute the Taylor coefficients (A.14) into series $F_{1,2}$ in Eqs. (A.8) and (A.9), and interchange the summations. In this way, the ascending series of the polylog (B.1) is recovered, so that

$$F_1\sim\lambda\sum_{n=0}^{\infty}\frac{\Gamma(n+1)}{\log^{n+1}\Lambda}\sum_{m=0}^{n}\delta^m\alpha_{n,m}(\lambda)\mathrm{Li}_{n+1-m}(-(1+\lambda)^{\delta}). \tag{A.16}$$

The expansion of F_2 is obtained from F_1 by changing the sign of δ and inserting the factor $(-1)^{n+1}$ into the n summation. The expansion of F_1+F_2 is thus

$$F_1+F_2\sim\lambda\sum_{n=0}^{\infty}\frac{n!}{\log^{n+1}\Lambda}\sum_{m=0}^{n}\delta^m\alpha_{n,m}(\lambda)\Delta_{n+1-m}((1+\lambda)^{\delta}), \tag{A.17}$$

where Δ_n are polynomials in $\delta\log(1+\lambda)$ as defined in Eqs. (B.11) and (B.12), and the coefficients $\alpha_{n,m}(\lambda)$ are defined by the finite series (A.15). By making use of (B.16) and (B.19), we calculate $\alpha_{n,m}(\lambda)$ for $n=0,1,2$:

$$\begin{aligned}&\alpha_{0,0}(\lambda)=\gamma_1^b\rho^{-b}(1+\lambda)^{a+b},\\&\alpha_{1,0}=-\frac{\alpha_{0,0}\lambda}{1+\lambda}(a+b\rho^2),\qquad \alpha_{1,1}=-\frac{\alpha_{0,0}\lambda}{1+\lambda},\\&\alpha_{2,0}=\frac{\alpha_{0,0}\lambda^2}{2(1+\lambda)^2}(a(a-1)+b(2a+1)\rho^2+b(b-2)\rho^4),\\&\alpha_{2,1}=\frac{\alpha_{0,0}\lambda^2}{2(1+\lambda)^2}(2a-1+2b\rho^2),\qquad \alpha_{2,2}=\frac{\alpha_{0,0}\lambda^2}{2(1+\lambda)^2}.\end{aligned} \tag{A.18}$$

The first three orders of the asymptotic expansion of F_1+F_2 in Eq. (A.17) thus read

$$\begin{aligned}F_1+F_2\sim{}&\frac{\gamma_1^b}{\rho^b}(1+\lambda)^{a+b}\frac{\lambda}{\log\Lambda}\Big\{\Delta_1-\frac{1}{1+\lambda}\frac{\lambda}{\log\Lambda}[(a+b\rho^2)\Delta_2+\delta\Delta_1]\\&+\frac{1}{(1+\lambda)^2}\frac{\lambda^2}{\log^2\Lambda}[(a(a-1)+b(2a+1)\rho^2+b(b-2)\rho^4)\Delta_3\\&+(2a-1+2b\rho^2)\delta\Delta_2+\delta^2\Delta_1]+\ldots\Big\},\end{aligned} \tag{A.19}$$

where $\Delta_{k=1,2,3}$ stands for $\Delta_k((1+\lambda)^{\delta})$, cf. Eqs. (B.11) and (B.12), and ρ is defined in Eq. (A.12). We introduce $z=1+\lambda$ as expansion parameter (in ascending powers of $1/z$):

$$z=\frac{1}{\beta\gamma_1}\log(\gamma_1^{-\delta}\Lambda_0)=1+\frac{\log\Lambda}{\beta\gamma_1}, \tag{A.20}$$

where Λ_0 is the fugacity, cf. Eq. (A.1), and $\Lambda=\gamma_1^{-\delta}\mathrm{e}^{-\beta\gamma_1}\Lambda_0$, cf. Eq. (A.2). λ is positive since $\Lambda>1$ is required in Eqs. (A.3)–(A.6). In Eq. (A.19), we substitute $1+\lambda=z$ as well as

$$\frac{\lambda}{\log\Lambda}=\frac{1}{\beta\gamma_1},\qquad \rho=\left(1-\frac{1}{\gamma_1^2z^2}\right)^{-1/2}. \tag{A.21}$$

We also note, cf. Eq. (B.12), $\Delta_1=-\delta\log z$, and

$$\Delta_2=-\frac{\delta^2}{2}\log^2 z-\frac{\pi^2}{6},\qquad \Delta_3=-\frac{\delta^3}{6}\log^3 z-\frac{\pi^2}{6}\delta\log z. \tag{A.22}$$

Expansion (A.19) is in ascending powers of $1/(\beta\gamma_1 z)$, and holds for arbitrary exponents a,b, and $\gamma_1\geq 1$, provided that $\beta\gamma_1 z\gg 1$. If in addition $\gamma_1 z\gg 1$, we can also expand ρ in Eq. (A.21) to find

$$\begin{aligned}F_1+F_2=\frac{(z\gamma_1)^{a+b}}{\gamma_1^{a+1}\beta}\Big\{&\Delta_1-\frac{1}{z\beta\gamma_1}[(a+b)\Delta_2+\delta\Delta_1]\\&+\frac{1}{(z\beta\gamma_1)^2}\Big[(a+b)(a+b-1)\Delta_3+(2a+2b-1)\delta\Delta_2\\&+\Big(\delta^2-\frac{b}{2}\beta^2\Big)\Delta_1\Big]+\mathrm{O}(z^{-3}\log^4 z)\Big\}.\end{aligned} \tag{A.23}$$

For this expansion to be valid, $\beta\gamma_1 z\gg 1$ as well as $\gamma_1 z\gg 1$ is required. That is, both conditions have to be met in a systematic $1/z$ expansion, where z is related to the fugacity $\Lambda_0=\mathrm{e}^{-\alpha}$ as stated in Eq. (A.20).

A.2. Zero-temperature degeneracy

In the zero-temperature limit, the contribution F_1+F_2 to the Fermi integral $F(a,b)$ in Eq. (A.1) vanishes, cf. Eqs. (A.19) and (A.23), so that F reduces to the temperature-independent residual $\gamma_1^{a+1}F_0$, cf. Eq. (A.3). We substitute $1+y=\sqrt{1+t}$ into F_0 in Eq. (A.3), and rescale t to find

$$F_0(a,b)=\frac{\gamma_1^b}{2}\hat\lambda^{a+b+1}\int_0^1\left(\frac{1}{\hat\lambda^2}+t\right)^{(a-1)/2}\left(\frac{\upsilon_1^2}{\hat\lambda^2}+t\right)^{b/2}\mathrm{d}t, \tag{A.24}$$

$$\hat\lambda:=\sqrt{(1+\lambda)^2-1},\qquad \upsilon_1:=\sqrt{1-1/\gamma_1^2}. \tag{A.25}$$

We consider the limit $\lambda\to\infty$, and expand F_0 in ascending powers of $1/\hat\lambda$. To this end, we split the integral (A.24) into $\int_0^\infty-\int_1^\infty$, and write $F_0=I_0^1=I_0^\infty-I_1^\infty$, where I stands for the right-hand side of Eq. (A.24) with lower and upper integration boundaries as indicated. Apparently, $\hat\lambda$ scales out in I_0^∞:

$$I_0^\infty=-\frac{\gamma_1^b}{a+b+1}\,{}_2F_1\left(-\frac{b}{2},-\frac{a+b+1}{2};\frac{1-a-b}{2};\frac{1}{\gamma_1^2}\right). \tag{A.26}$$

In the integrand of I_1^∞, we expand both factors in ascending powers of $1/t$, and use term-by-term integration:

$$I_1^\infty=-\gamma_1^b\hat\lambda^{a+b+1}\sum_{n=0}^\infty\frac{c_n}{a+b+1-2n}\,\frac{1}{\hat\lambda^{2n}}, \tag{A.27}$$

$$c_n:=\sum_{k=0}^n\upsilon_1^{2k}\frac{(b/2)_k}{k!}\,\frac{((a-1)/2)_{n-k}}{(n-k)!}, \tag{A.28}$$

where $(a)_n$ denotes the falling factorial, $a(a-1)\ldots(a-n+1)$. The ascending $1/\hat\lambda^2$ expansion of F_0 in Eq. (A.24) is thus obtained as $F_0=I_0^\infty-I_1^\infty$, with series (A.26) and (A.27) substituted. In the case of integer exponents a and b, singularities can arise in the series coefficients of I_0^∞ and I_1^∞, which cancel if ε expanded, cf. Eq. (A.30).

We consider the special case $\gamma_1=1$, that is $\upsilon_1=0$ in Eq. (A.24). Here, $b>-2$ is necessary for integral (A.24) to converge,

$$F_0(a,b,\gamma_1=1)=\frac{\Gamma((b+2)/2)\Gamma(-(a+b+1)/2)}{2\Gamma((1-a)/2)}+\frac{\hat\lambda^{a+b+1}}{a+b+1}\,{}_2F_1\left(\frac{1-a}{2},-\frac{a+b+1}{2};\frac{1-a-b}{2};-\frac{1}{\hat\lambda^2}\right). \tag{A.29}$$

This can directly be obtained from Eq. (A.24) via the decomposition $\int_0^\infty-\int_1^\infty$or from Eqs. (A.26)–(A.28), the first term on the right-hand side in Eq. (A.29) being $I_0^\infty(\gamma_1=1)$ and the second $-I_1^\infty(\gamma_1=1)$. A singularity may occur in the first term due to a pole of the second gamma function in the nominator. A corresponding singularity arises in a series coefficient of the hypergeometric term, so that the singularities cancel if ε expanded [17]. The poles occur at $a=2k-1-b$, $k=0,1,2,\ldots$, for arbitrary real $b>-2$; we find $F_0(\gamma_1=1,a=2k-1-b)$ as

$$F_0=\frac{(-1)^k}{2}\,\frac{(b/2)_k}{k!}(2\log\hat\lambda+\psi(k+1)-\psi(b/2+1))+\frac{\hat\lambda^{2k}}{2}\sum_{\substack{n=0\\n\neq k}}^\infty\frac{(-b/2-1+k)_n}{n!(k-n)}\,\frac{1}{\hat\lambda^{2n}}, \tag{A.30}$$

where ψ is the logarithmic derivative of the gamma function. The asymptotic expansion of the Fermi integral $F(a,b)=\gamma_1^{a+1}(F_0+F_1+F_2)$ in Eqs. (A.1) and (A.3) is assembled with F_1+F_2 in Eq. (A.17) and $F_0=I_0^\infty-I_1^\infty$ in Eqs. (A.26)–(A.28). In the case that F is complete, with lower integration boundary $\gamma_1=1$, we can use F_0 in Eq. (A.29) or (A.30).

We list the integrals $F_0(a,b)$ (defined in Eq. (A.24)) occurring in the thermodynamic functions (2.3)–(2.5). As in Eq. (A.20), we put $z=1+\lambda$, so that $\hat\lambda^2=z^2-1$, cf. Eq. (A.25), and obtain by elementary integration of Eq. (A.24),

$$F_0(-1,1)=\gamma_1 z\sqrt{1-\frac{1}{\gamma_1^2z^2}}-\gamma_1\sqrt{1-\frac{1}{\gamma_1^2}}+\arcsin\frac{1}{\gamma_1 z}-\arcsin\frac{1}{\gamma_1},$$

$$F_0(0,1)=\frac{1}{2\gamma_1}\left[\gamma_1^2z^2\sqrt{1-\frac{1}{\gamma_1^2z^2}}-\gamma_1^2\sqrt{1-\frac{1}{\gamma_1^2}}-(\operatorname{arccosh}(\gamma_1 z)-\operatorname{arccosh}\gamma_1)\right],$$

$$F_0(1,1)=\frac{1}{3\gamma_1^2}\left[\gamma_1^3z^3\left(1-\frac{1}{\gamma_1^2z^2}\right)^{3/2}-\gamma_1^3\left(1-\frac{1}{\gamma_1^2}\right)^{3/2}\right],$$

$$F_0(2,1)=\frac{1}{4\gamma_1^3}\left[\gamma_1^4z^4\sqrt{1-\frac{1}{\gamma_1^2z^2}}-\gamma_1^4\sqrt{1-\frac{1}{\gamma_1^2}}-\frac{1}{2}\left(\gamma_1^2z^2\sqrt{1-\frac{1}{\gamma_1^2z^2}}-\gamma_1^2\sqrt{1-\frac{1}{\gamma_1^2}}\right)-\frac{1}{2}(\operatorname{arccosh}(\gamma_1 z)-\operatorname{arccosh}\gamma_1)\right], \tag{A.31}$$

where $0<\arcsin<\pi/2$, $z>1$, and $\gamma_1\geq 1$. The partition function (2.5) is assembled from

$$F_0(-1,3)=\gamma_1^2F_0(1,1)-F_0(-1,1),\qquad F_0(0,3)=\gamma_1^2F_0(2,1)-F_0(0,1), \tag{A.32}$$

and there is also a zero-temperature contribution from F_1+F_2 via $\beta F(0,3)$, cf. Eq. (A.38). The spectral functions (4.10) are compiled at $b=0$, where

$$F_0(a,0)=\frac{z^{1+a}-1}{1+a},\quad F_0(-1,0)=\log z, \tag{A.33}$$

which is independent of γ_1, cf. Eq. (A.24).

We consider $\gamma_1=1$ and expand Eqs. (A.31) and (A.32) in $1/z$ to find

$$F_0(-1,1)=z-\frac{\pi}{2}+\frac{1}{2}\,\frac{1}{z}+\frac{1}{24}\,\frac{1}{z^3}+\mathrm{O}(z^{-5}),$$

$$F_0(0,1)=\frac{1}{2}z^2-\frac{1}{2}\log(2z)-\frac{1}{4}+\frac{1}{16}\,\frac{1}{z^2}+\mathrm{O}(z^{-4}),$$

$$F_0(1,1)=\frac{1}{3}z^3-\frac{1}{2}z+\frac{1}{8}\,\frac{1}{z}+\frac{1}{48}\,\frac{1}{z^3}+\mathrm{O}(z^{-5}),$$

$$F_0(2,1)=\frac{1}{4}z^4-\frac{1}{4}z^2-\frac{1}{8}\log(2z)+\frac{1}{32}+\frac{1}{32}\,\frac{1}{z^2}+\mathrm{O}(z^{-4}),$$

$$F_0(-1,3)=\frac{1}{3}z^3-\frac{3}{2}z+\frac{\pi}{2}-\frac{3}{8}\,\frac{1}{z}-\frac{1}{48}\,\frac{1}{z^3}+\mathrm{O}(z^{-5}),$$

$$F_0(0,3)=\frac{1}{4}z^4-\frac{3}{4}z^2+\frac{3}{8}\log(2z)+\frac{9}{32}-\frac{1}{32}\,\frac{1}{z^2}+\mathrm{O}(z^{-4}). \tag{A.34}$$

Here, $\gamma_1=1$ is implied, but γ_1 can readily be scaled into these series according to Eqs. (A.31) and (A.32), so that the expansions are in ascending powers of $1/(\gamma_1 z)$. Eqs. (A.31)–(A.33) give the fully degenerate contribution $F_0(a,b)$ to the Fermi integral (A.1)–(A.3). The fugacity expansion (A.34) of F_0 is needed even though the exact result (A.31) and (A.32) is known, since we have to iteratively solve for z when calculating the thermodynamic variables, cf. Section 3.

A.3. Number count, internal energy, and partition function in the nearly degenerate regime

The fugacity expansion of the Fermi integral $F(a,b,\gamma_1=1)$ in Eq. (A.1) is obtained by adding F_1+F_2 in Eq. (A.23) (with $\gamma_1=1$) and F_0 in Eq. (A.34). We find, for exponents $a=b=1$:

$$F(1,1)=\frac{z^3}{3}\left\{1-\frac{3\delta}{\beta z}\log z+\frac{3}{(\beta z)^2}\left(\delta^2\log^2 z+\delta^2\log z+\frac{\pi^2}{3}-\frac{b}{2}\beta^2\right)-\frac{3\delta}{(\beta z)^3}\left[\frac{1}{3}\delta^2\log^3 z+\frac{3}{2}\delta^2\log^2 z+\left(\delta^2+\frac{\pi^2}{3}-\frac{b}{2}\beta^2\right)\log z+\frac{\pi^2}{2}\right]+\ldots\right\}, \tag{A.35}$$

where we have to put $b=1$ in the $1/z^2$ and $1/z^3$ terms. The expansion of $F(-1,3)$ is likewise given by Eq. (A.35) with $b=3$, and

$$F(2,1)=\frac{z^4}{4}\left\{1-\frac{4\delta}{\beta z}\log z+\frac{4}{(\beta z)^2}\left(\frac{3}{2}\delta^2\log^2 z+\delta^2\log z+\frac{\pi^2}{2}-\frac{b}{4}\beta^2\right)-\frac{4\delta}{(\beta z)^3}\left[\delta^2\log^3 z+\frac{5}{2}\delta^2\log^2 z+\left(\delta^2+\pi^2-\frac{b}{2}\beta^2\right)\log z+\frac{5}{6}\pi^2\right]+\ldots\right\}, \tag{A.36}$$

with $b=1$. The latter is also the expansion of $F(0,3)$, if we put $b=3$ in the third and fourth term. The ellipses in Eqs. (A.35) and (A.36) stand for terms of $O(z^{-4}\log^4 z)$. Expansions (A.35) and (A.36) of the Fermi integral $F(a,b,\gamma_1=1)$ in Eq. (A.1) apply for $z\beta=\log\Lambda_0\gg 1$ and $z\gg 1$. The parameter Λ_0 in Eq. (A.1) is identified with the fugacity $e^{-\alpha}$, which is related to the chemical potential by $\alpha=-\beta\mu/m$, where $\beta=m/(kT)$. Hence, if $\gamma_1=1$, we can identify $z=\mu/m$, cf. Eq. (A.20).

The fugacity expansions of the particle number and the internal energy read, cf. Eqs. (2.3), (2.4), and (A.1),

$$N=\frac{m^3V}{\pi^2}F(1,1),\qquad U=\frac{m^4V}{\pi^2}F(2,1), \tag{A.37}$$

with series (A.35) and (A.36) substituted. The expansion of the partition function $\log Z$ in Eq. (2.5) ($\gamma_1=1$) is assembled as

$$\frac{\log Z}{m^3V}=\frac{1}{3\pi^2}(\beta F(0,3)+\delta F(-1,3))=\frac{\beta z^4}{12\pi^2}\left\{1-\frac{4\delta}{\beta z}\left(\log z-\frac{1}{3}\right)+\frac{4}{(\beta z)^2}\left(\frac{3}{2}\delta^2\log^2 z+\frac{\pi^2}{2}-\frac{3}{4}\beta^2\right)-\frac{4\delta}{(\beta z)^3}\left[\delta^2\log^3 z+\frac{3}{2}\delta^2\log^2 z+\left(\pi^2-\frac{3}{2}\beta^2\right)\log z+\frac{1}{2}\pi^2+\frac{3}{2}\beta^2\right]+\ldots\right\}. \tag{A.38}$$

Here, $F(0,3)$ is series (A.36), and $F(-1,3)$ series (A.35), both with $b=3$. The ellipsis stands for terms of $O((\beta z)^{-4}\log^4 z)$.

Appendix B. Polylogarithms, Stirling numbers, and Gegenbauer polynomials

To keep this article self-contained, we summarize some technical concepts as well as the notation used in the expansion of the Fermi integrals in Appendix A. We start with the series representation of the polylogarithm [40–47]:

$$\mathrm{Li}_s(z):=\sum_{n=1}^{\infty}\frac{z^n}{n^s}, \tag{B.1}$$

which converges in the unit disk $|z|<1$ for arbitrary complex integer s, and admits analytic continuation by means of the integral representations [43,44]:

$$\mathrm{Li}_s(z)=\frac{-1}{\Gamma(s-1)}\int_0^1|\log t|^{s-2}\log(1-zt)\frac{\mathrm{d}t}{t}=\frac{z}{\Gamma(s)}\int_1^{\infty}\frac{\log^{s-1}t}{t(t-z)}\mathrm{d}t=\frac{1}{\Gamma(s)}\int_0^{\infty}\frac{t^{s-1}\,\mathrm{d}t}{z^{-1}e^t-1}. \tag{B.2}$$

The first integral converges in the half-plane $\mathrm{Re}(s)>1$, the second and third require $\mathrm{Re}(s)>0$; otherwise they are identical via partial integration and obvious substitutions. Series (B.1) is recovered by expansion in ascending powers and term-by-term integration. Fermi–Dirac integrals are defined by the third representation in Eq. (B.2), as $-\Gamma(s)\mathrm{Li}_s(-z)$.

We note $\mathrm{Li}_s(-1)=(2^{1-s}-1)\zeta(s)$; in particular, $\mathrm{Li}_1(-1)=-\log 2$ and $\mathrm{Li}_2(-1)=-\pi^2/12$. We will mainly consider real negative z or at least $z<1$. $\mathrm{Li}_s(z)$ is analytic in the z plane with branch cut $(1,\infty)$ along the positive real axis, except for $s=0$ and at negative integer s, where the polylogs are rational functions, obtained by recursive differentiation of $\mathrm{Li}_1(z)=-\log(1-z)$ according to

$$\left(z\frac{\mathrm{d}}{\mathrm{d}z}\right)^k\mathrm{Li}_s(z)=\mathrm{Li}_{s-k}(z),\qquad \mathrm{Li}_s(z)=\int_0^z\mathrm{Li}_{s-1}(t)\frac{\mathrm{d}t}{t}. \tag{B.3}$$

The asymptotic expansion for large negative z is obtained from Jonquière's inversion formula [48]:

$$\mathrm{Li}_s(-r)+e^{i\pi s}\mathrm{Li}_s\left(-\frac{1}{r}\right)=\frac{(2\pi)^s}{\Gamma(s)}e^{i\pi s/2}\zeta\left(1-s,\frac{1}{2}-i\frac{\log r}{2\pi}\right), \tag{B.4}$$

where

$$\zeta(s,z):=\sum_{n=0}^{\infty}\frac{1}{(n+z)^s} \tag{B.5}$$

is the Hurwitz zeta function, and $r>0$ is implied in Eq. (B.4). $\zeta(s,z)$ admits the integral representation [48]:

$$\zeta\left(s,\frac{1}{2}+z\right)=\frac{1}{\Gamma(s)}\int_0^{\infty}\frac{e^{-zt}t^{s-1}\,\mathrm{d}t}{e^{t/2}-e^{-t/2}}, \tag{B.6}$$

from which the large-z asymptotics is obtained by substituting the generating series of the Bernoulli numbers:

$$\frac{te^{t/2}}{e^t-1}=\sum_{k=0}^{\infty}\frac{B_k(1/2)}{k!}t^k,\qquad B_k\left(\frac{1}{2}\right):=(2^{1-k}-1)B_k, \tag{B.7}$$

and using term-by-term integration (which amounts to applying Fourier asymptotics or Watson's lemma if the integration path is rotated into the imaginary axis [40]). The $r\to\infty$ asymptotics of the inversion formula (B.4) is thus found as [47]:

$$\mathrm{Li}_s(-r)+e^{i\pi s}\mathrm{Li}_s\left(-\frac{1}{r}\right)\sim-\frac{\log^s r}{\Gamma(1+s)}\left(1-2\sum_{k=1}^{\infty}\mathrm{Li}_{2k}(-1)\frac{(s)_{2k}}{\log^{2k}r}\right), \tag{B.8}$$

where

$$\mathrm{Li}_{2k}(-1)=(-1)^k(1-2^{1-2k})\frac{(2\pi)^{2k}}{2(2k)!}B_{2k}, \tag{B.9}$$

$$(s)_{2k}=\frac{\Gamma(2k-s)}{\Gamma(-s)}=\frac{\Gamma(1+s)}{\Gamma(1+s-2k)}. \tag{B.10}$$

Here, $(s)_n$ is the falling factorial $s(s-1)\ldots(s-n+1)$, not to be confused with the Pochhammer symbol or rising factorial $(s)^{(n)}:=s(s+1)\ldots(s+n-1)$, so that $(s)_n=(-1)^n(-s)^{(n)}$.

The second polylog on the left-hand side of Eq. (B.8) can be dropped, $e^{i\pi s}\mathrm{Li}_s(-1/r)=O(1/r)$, as terms of this order have been discarded in the expansion procedure. However, the asymptotic

series terminates for integer $s \geq 0$, and then Eq. (B.8) holds true as an identity even for small r. In the case of negative integer s, the right-hand side of Eq. (B.8) vanishes due to the poles of $\Gamma(1+s)$ in the denominator. In Eq. (B.8), we put $s = n = 0, 1, 2, \ldots$ to find [42]

$$\Delta_n(r) := \mathrm{Li}_n(-r) + (-1)^n \mathrm{Li}_n\left(-\frac{1}{r}\right) = -\frac{1}{n!}\log^n r + 2\sum_{k=1}^{[n/2]} \mathrm{Li}_{2k}(-1)\frac{\log^{n-2k} r}{(n-2k)!}. \tag{B.11}$$

This can also directly be obtained from Eq. (B.4), since $\zeta(1-s,z)$ reduces to a Bernoulli polynomial for positive integer s [48]. We note $\Delta_1(r) = -\log r$ as well as the inversion formulas of the di- and trilogarithm:

$$\Delta_2(r) = -\frac{1}{2}\log^2 r - \frac{\pi^2}{6}, \quad \Delta_3(r) = -\frac{1}{6}\log^3 r - \frac{\pi^2}{6}\log r. \tag{B.12}$$

Apparently $\Delta_n(1/r) = (-1)^n \Delta_n(r)$. Finally, multiple s differentiation of $\Gamma(s)\mathrm{Li}_s(z)$ amounts to adding a factor of $\log^k t$ to the integrand of the third (Fermi–Dirac) integral in Eq. (B.2). The series expansions of these integrals are obtained via term-by-term differentiation of the ascending series (B.1) and the asymptotic expansion (B.8).

In Appendix A, we also need the polynomial expansion of the falling factorial:

$$(k)_n = n!\binom{k}{n} = \sum_{m=0}^{n} S_{n,m} k^m, \tag{B.13}$$

where k is real and $S_{n,m}$, $0 \leq m \leq n$, are Stirling numbers of the first kind [49]. In particular, $S_{n,0} = 0$ for $n > 0$, and $S_{n,n} = 1$, as well as $S_{n,1} = (-1)^{n-1}(n-1)!$ and $S_{n,n-1} = -n(n-1)/2$. It is convenient to put $S_{n,m} = 0$ for $m > n$, so that $S_{n,m}$ is defined for all non-negative integers n and m, and the summation in Eq. (B.13) can be extended to infinity. In Eq. (A.15), we use an expansion slightly more general than (B.13):

$$\frac{(k\delta + a)_n}{n!} = \sum_{j=0}^{n} \frac{(a)_j}{j!}\frac{(k\delta)_{n-j}}{(n-j)!} = \sum_{m=0}^{n} S(n,m;a)\delta^m k^m, \tag{B.14}$$

$$S(n,m;a) := \sum_{j=0}^{n-m} \frac{(a)_j}{j!}\frac{S_{n-j,m}}{(n-j)!}, \tag{B.15}$$

where k, δ, and a are arbitrary real numbers. In particular, $S(n,m;0) = S_{n,m}/n!$, and we define $S(n,m;a) = 0$ if $m > n$. For $n = 0, 1, 2$, coefficients (B.15) read

$$S(0,0;a) = 1, \quad S(1,0;a) = a, \quad S(1,1;a) = 1,$$

$$S(2,0;a) = \tfrac{1}{2}a(a-1), \quad S(2,1;a) = a - \tfrac{1}{2}, \quad S(2,2;a) = \tfrac{1}{2}. \tag{B.16}$$

In Eq. (A.13), we use an expansion in Gegenbauer polynomials, based on the generating series [48]:

$$(t^2 - 2\rho t + 1)^{\alpha} = \sum_{n=0}^{\infty} C_n^{(-\alpha)}(\rho) t^n. \tag{B.17}$$

Splitting the left-hand side into two factors $(1 - t/\rho_{\pm})^{\alpha}$, $\rho_{\pm} := \rho \pm \sqrt{\rho^2 - 1}$, we see that the expansion is absolutely convergent for $|t| < \min(|\rho_{\pm}|)$ and arbitrary ρ. More explicitly

$$C_n^{(\lambda)}(x) = \sum_{k=0}^{[n/2]} \frac{(-1)^k (\lambda)^{(n-k)}}{k!(n-2k)!} 2^{n-2k} x^{n-2k}, \tag{B.18}$$

where $(\lambda)^{(n)}$ is the Pochhammer symbol $\Gamma(\lambda+n)/\Gamma(\lambda)$. We note

$$C_0^{(\lambda)}(x) = 1, \quad C_1^{(\lambda)}(x) = 2\lambda x, \quad C_2^{(\lambda)}(x) = 2\lambda(\lambda+1)x^2 - \lambda. \tag{B.19}$$

Gegenbauer polynomials are a special class of hypergeometric polynomials,

$$C_{2n}^{(\lambda)}(x) = (-1)^n \frac{(\lambda)^{(n)}}{n!} {}_2F_1(-n, n+\lambda; 1/2; x^2),$$

$$C_{2n+1}^{(\lambda)}(x) = (-1)^n (\lambda)^{(n+1)} \frac{2x}{n!} {}_2F_1(-n, n+\lambda+1; 3/2; x^2). \tag{B.20}$$

At $\lambda = 1/2$, they coincide with the Legendre polynomials $P_n(x)$, and at $\lambda = 1$ with the Chebyshev polynomials of the second kind $U_n(x)$ [48]. Finally, $C_n^{(\lambda)}(1) = (2\lambda)^{(n)}/n!$, $C_n^{(\lambda)}(-x) = (-1)^n C_n^{(\lambda)}(x)$, and $C_{n\geq 1}^{(0)}(\rho) = 0$.

References

[1] R.F. Elsner, et al., Icarus 178 (2005) 417.
[2] R. Tomaschitz, Physica A 387 (2008) 3480.
[3] R. Tomaschitz, Opt. Commun. 282 (2009) 1710.
[4] S. Tanaka, Prog. Theor. Phys. 24 (1960) 171.
[5] R. Newton, Science 167 (1970) 1569.
[6] G. Feinberg, Sci. Am. 222 (1970) 69.
[7] K. Kamoi, S. Kamefuchi, Prog. Theor. Phys. 45 (1971) 1646.
[8] R. Tomaschitz, Eur. Phys. J. B 17 (2000) 523.
[9] B.M. Bolotovskiĭ, V.L. Ginzburg, Sov. Phys. Usp. 15 (1972) 184.
[10] B.M. Bolotovskiĭ, V.P. Bykov, Sov. Phys. Usp. 33 (1990) 477.
[11] A.V. Bessarab, et al., IEEE Trans. Plasma Sci. 32 (2004) 1400.
[12] A.V. Bessarab, et al., Radiat. Phys. Chem. 75 (2006) 825.
[13] H. Ardavan, et al., J. Opt. Soc. Am. A 24 (2007) 2443.
[14] H. Ardavan, et al., J. Opt. Soc. Am. A 25 (2008) 543.
[15] M.S. Bigelow, N.N. Lepeshkin, R.W. Boyd, Science 301 (2003) 200.
[16] T. Baba, Nature Photon. 2 (2008) 465.
[17] G.M. Gehring, et al., Science 312 (2006) 895.
[18] L. Thévenaz, Nature Photon. 2 (2008) 474.
[19] G. Dolling, et al., Science 312 (2006) 892.
[20] L. Brillouin, Wave Propagation and Group Velocity, Academic Press, New York, 1988.
[21] P.K. Chakraborty, S.K. Biswas, K.P. Ghatak, Physica B 352 (2004) 111.
[22] A. Minguzzi, M.P. Tosi, Physica B 300 (2001) 27.
[23] G. Branduardi-Raymont, et al., Planet. Space Sci. 55 (2007) 1126.
[24] R. Tomaschitz, Physica A 385 (2007) 558.
[25] J. Albert, et al., Astrophys. J. 663 (2007) 125.
[26] A. Konopelko, et al., Astrophys. J. 679 (2008) L13.
[27] R. Tomaschitz, EPL 85 (2009) 29001.
[28] D.A. Howell, et al., Nature 443 (2006) 308.
[29] I. Iben Jr., Phys. Rep. 250 (1995) 1.
[30] R. Tomaschitz, Phys. Lett. A 372 (2008) 4344.
[31] R. Tomaschitz, Eur. Phys. J. C 49 (2007) 815.
[32] R. Tomaschitz, Eur. Phys. J. D 32 (2005) 241.
[33] K.A. Kazakov, Physica B 403 (2008) 2255.
[34] R. Tomaschitz, Ann. Phys. 322 (2007) 677.
[35] R. Tomaschitz, EPL 84 (2008) 19001.
[36] J. Belz, et al., Nucl. Phys. B (Proc. Suppl.) 190 (2009) 5.
[37] R. Tomaschitz, Phys. Lett. A 366 (2007) 289.
[38] R. Tomaschitz, Physica B 404 (2009) 1383.
[39] S. Chandrasekhar, An Introduction to the Study of Stellar Structure, Dover, New York, 1967.
[40] E.T. Copson, Asymptotic Expansions, Cambridge University Press, Cambridge, 1965.
[41] C. Truesdell, Ann. Math. 46 (1945) 144.
[42] L. Lewin, Polylogarithms and Associated Functions, North-Holland, Amsterdam, 1981.
[43] K.S. Kölbig, J.A. Mignaco, E. Remiddi, BIT 10 (1970) 38.
[44] R. Barbieri, J.A. Mignaco, E. Remiddi, Nuovo Cimento A 11 (1972) 824.
[45] A. Devoto, D.W. Duke, Riv. Nuovo Cimento 7 (1984) 1.
[46] K.S. Kölbig, SIAM J. Math. Anal. 17 (1986) 1232.
[47] M.H. Lee, J. Math. Phys. 36 (1995) 1217.
[48] W. Magnus, F. Oberhettinger, R.P. Soni, Formulas and Theorems for the Special Functions of Mathematical Physics, Springer, New York, 1966.
[49] J. Riordan, Combinatorial Identities, Wiley, New York, 1968.